Frequency dependence of acoustic waves in marine sediments

G. Robb[a,b], A. I. Best[a], J. K. Dix[a], T. G. Leighton[b], A. Harris[a], J.S. Riggs[a], J. M. Bull[a], P. R. White[b]

[a]*Southampton Oceanograpy Centre, Southampton, SO14 6TZ, UK, e-mails: gbor199@soc.soton.ac.uk, aib@soc.soton.ac.uk, jkd@soc.soton.ac.uk, andy@soc.soton.ac.uk, jsr@soc.soton.ac.uk, bull@soc.soton.ac.uk.*
[b]*Institute of Sound and Vibrational Research, Southampton University, Southampton, SO17 1BJ, UK, e-mails: tgl@isvr.soton.ac.uk, prw@isvr.soton.ac.uk.*

Summary

In situ techniques provide the most reliable method of examining the geoacoustical properties of marine sediments. In the past, individual *in situ* surveys have only been able to examine compressional waves over a maximum frequency range of 100 Hz to 50 kHz. A new *in situ* acoustic device, the Sediment Probing Acoustic Detection Equipment, or SPADE, has been developed, which can emit a variety of pulses, e.g. tonal and swept-frequency, over a continuous frequency range of 10 - 100 kHz. Data from a recent field trial are analysed to obtain the *in situ* velocity and attenuation over frequency increments of 5 kHz between 10 - 75 kHz. Results imply that scattering is a dominant attenuation mechanism from 10-75 kHz and the media is dispersive for frequencies between 60 and 70 kHz and below 20 kHz. Biot theory cannot accurately model the observed velocity and attenuation.

1. Introduction

Detailed knowledge of the frequency dependence of the compressional wave velocity and attenuation in sediments is important to a number of marine fields, e.g. seafloor stability hazard assessment and military sonar performance studies. *In situ* surveys provide the most reliable method of investigating these relationships, with any outcomes being directly applicable to the "undisturbed" sediment under examination. Laboratory acoustic measurements on geological samples may not be representative of *in situ* properties because of small sample sizes and unknown disturbance of the sample. Acoustic measurements obtained from reflection/refraction profiling also possess uncertainties, arising from variable degrees of reflection/scattering occurring at impedance boundaries.

A number of authors have published measurements of compressional wave velocity and attenuation, which have been obtained using *in situ* devices. Early work typically used explosive charges as sources, hence limiting the range of central frequencies to under 1 kHz, [1-5]. Additional acoustic sources have also been used to examine this sub kHz range [6-8].

A wide suite of the data present in literature is limited to specific frequencies. This data examines seafloor sediments at frequencies of: 100 kHz [9], 25 kHz [10], 14, 7 and 3.5 kHz [11], 250 kHz and 1 kHz [12] and 38 and 58 kHz, using ISSAMS [13-15], and NEPTUNE [13, 14]. In addition deep-sea sediments have been investigated, during coring, at frequencies of 190 kHz [16] and 200 kHz [17].

A number of authors measured the *in situ* velocity and attenuation over a range of frequencies. The earliest of these investigated marine muds from 4 - 50 kHz [18], utilizing only 5 discrete frequencies in this range. The frequency range of 5 - 50 kHz is re-examined for sands/silts from land/beach environments [19] and shallow water sediments [12]. Turgut and Yamamoto use a variety of sources to examine saturated beach sediments at frequencies from 1 - 30 kHz [20], using minimum frequency increments of approximately 3 kHz. An acoustic LANCE uses a broadband source, with a frequency content of 5 - 20 kHz for vertical deployments, to examine marine sediments down to 4 m below the seabed [13, 21]. Recent work, based at Southampton Oceanography Centre, has focused on 1 - 10 kHz,

using such broadband sources as the mini-boomer [22, 23] and SAPPA [24].

During September - November, 1999, a series of high frequency sediment acoustics experiments, SAX99, were carried out on shallow water sediments. Though these focused on backscatter measurements, compressional wave velocity and attenuation were investigated, using *in situ* probes, for frequencies up to 300 kHz. However, for frequencies over 50 kHz, preliminary calculations of velocity and attenuation displayed large fluctuations, possibly due to scattering from shells [25]. To date *in situ* velocities and attenuations arising from SAX99 have only been published for frequencies less than 50 kHz [26].

In summary the relatively few studies of *in situ* compressional wave velocities and attenuations either use a limited frequency range, or a limited range of sediment types. In addition, owing to the range of sources and receivers used, direct comparison of results from different surveys may not be possible.

2. The SPADE

The SPADE (Sediment Probing Acoustic Detection Equipment) is able to systematically examine the compressional wave velocity and attenuation of marine sediments, down to 2 m below the seafloor, over the frequency range of 10 – 100 kHz. It is able to produce acoustic pulses, with any central frequency between 10-100 kHz. In addition a variety of pulses, e.g. tonal or swept-frequency, can be emitted. The SPADE consists of a portion of piezoceramic, with a convex emitting face, Fig. 1a. The dimensions of the ceramic are 0.2 m by 0.12 m. The convex emitting face produces a radial beam, with a fan-like appearance in the horizontal plane.

The current receiver, Fig. 1b, consists of an air backed hemispherical barium titanate transducer, with a width of approximately 15 mm, diameter of 32 mm and a resonant frequency of 80 kHz, the effects of which are minimised electronically. For easy insertion and deployment, both the SPADE and receiver are mounted in 2 m long aluminium channels. The receiver is embedded in a silicone elastomer to allow acoustic coupling to the sediment.

Digital pulses are generated in software. These are converted into analogue pulses before being amplified by a custom-built pulse power amplifier, which is capable of driving the transducer over the frequency range of 10-100 kHz at peak-to-peak voltages of 50-200 V.

For the field trials presented in this paper, tonal pulses were used. Typical pulses are displayed in Figure 2. Each pulse contains a maximum of 10 oscillations, modulated with a cosine-squared envelope. For 15-100 kHz this modulation acted to minimise the sidelobes to less than 5% the amplitude of central frequency. The *bandwidth* of the emitted waves ranged from approximately 5 kHz at a central frequency of 10 kHz to 40 kHz at a central frequency of 100 kHz. The examination of transmitted signals received during field trials confirm that the acoustic pulse emitted from the SPADE is essentially a scaled version of the analogue pulse sent to the transducer, the degree of scaling depending on the frequency response of the SPADE, Fig. 2d. Small tail effects are a result of electronic ringing. As no time lag occurs across the transducer, this electronic pulse is considered to accurately reflect the shape of, and be in phase with, the acoustic pulse emitted.

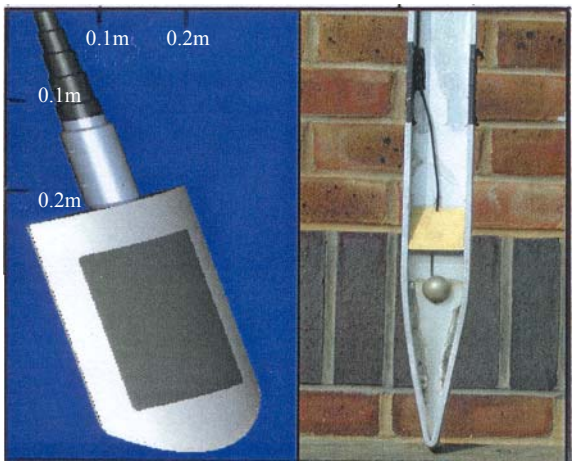

Figure 1. The SPADE (a) and receiver (b), on same scale.

3. Field trials

Field trials were performed on inter-tidal sediment at Hastings beach, West Sussex (National Grid Reference TQ 782 085). The sediment appeared to consist of homogeneous, isotropic sand which, for sediment depths of 20 cm or greater, remained fully saturated throughout the entire tidal cycle. Field data was collected from uncovered sediments during the low tide period on the 5th March, 2002.

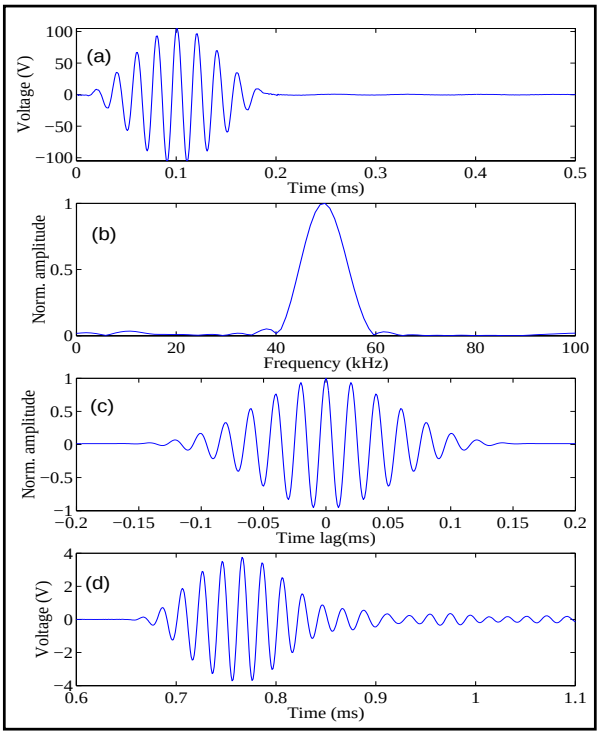

Figure 2. Typical pulses at 50 kHz: (a) electronic pulse sent to SPADE transducer with a peak-to-peak voltage of 200 V; (b) its frequency content; (c) its auto-correlation; (d) a typical pulse received during field trials.

The following experimental procedure was employed. The SPADE was placed at a sediment depth of 0.65 m. The receiver was then placed, at the same depth, in a line perpendicular to the face of the SPADE, i.e. in the centre of the wave-field emitted by the SPADE. An initial source to receiver, S-R, separation of 3.9 m was used. Utilising pulses with peak-to-peak voltages of 200 V, five shots were fired at each of 19 frequencies over the range of 10-100 kHz, at increments of 5 kHz. For each shot both the electronic pulse discussed earlier and received signal were recorded using a sampling frequency of 1 MHz.

The receiver was then moved to S-R separations of 3.5, 3.0, 2.43, 1.8, 1.38, 1.01 m and identical shots fired. This approach was used to minimise sediment disturbance. In addition background noise was recorded and sediment samples collected. Errors of 1 cm are expected in measurements of depth and S-R separation.

4. Data analysis and results

The following analysis uses the arrival time and amplitude of the directly transmitted wave to measure the compressional wave velocity and attenuation of the sediment. It assumes isotropic, homogeneous sediment. Athough our analysis does not require knowledge of the frequency response of the emitting or receiving transducers these responses will result in a frequency dependent signal to noise ratio, SNR. This will be resolved in future work.

Butterworth high-pass filters were routinely applied to the acquired data to attenuate low frequency, less than 15 kHz, environmental and electronic noise. The properties of these filters were adapted to suit the central frequency of the emitted wave, i.e. to allow maximum attenuation of low frequency noise while retaining the entirety of the signal originating from the SPADE. SNRs were further improved by stacking the filtered signals at each frequency and S-R separation, Fig.3.

Only received signals that displayed good SNRs and clearly resolved transmitted pulses were used in the following analysis. As signals at 80 kHz or greater were only received at the smallest S-R separation, velocity and attenuation could only be calculated from 10 - 75 kHz. Future work will use S-R separations less than 1 m to allow the 80 - 100 kHz region to be examined.

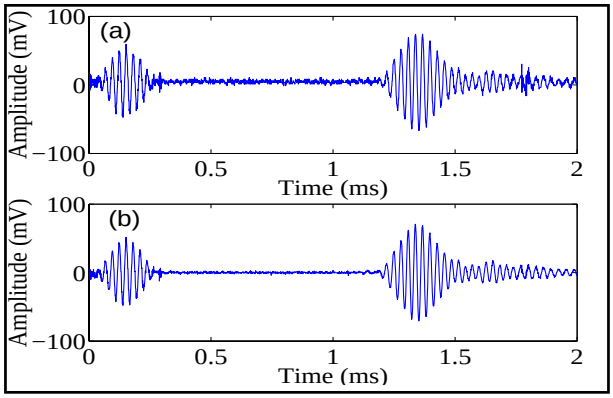

Figure 3. Signals received at 35 kHz and 1.8 m S-R separation: (a) raw signal; (b) normalized stacked and filtered signal. The directly transmitted pulse (centered on 1.35 ms), electronic break-through (centered on 0.15 ms) and additional pulses (commencing at 1.45 ms) can all be observed.

In order to calculate the frequency dependent velocity the stacked-filtered-received signal was correlated with the corresponding electronic pulse, the use of which has been previously justified. The arrival time of the directly transmitted wave corresponds to the peak of the correlated signal. However, as the auto-correlation of the electronic pulse possesses a smooth envelope, Fig. 2c, this peak can be difficult to resolve. In such cases arrival time data were omitted from the subsequent velocity determination. For each frequency the S-R

separation was plotted against the arrival time and a least squares linear fit applied, the gradient of which represents the velocity, Fig. 4. Figure 5 displays the frequency dependent velocity, with errors calculated using standard statistical analysis for 95% confidence limits and all points based on three or more valid arrival times.

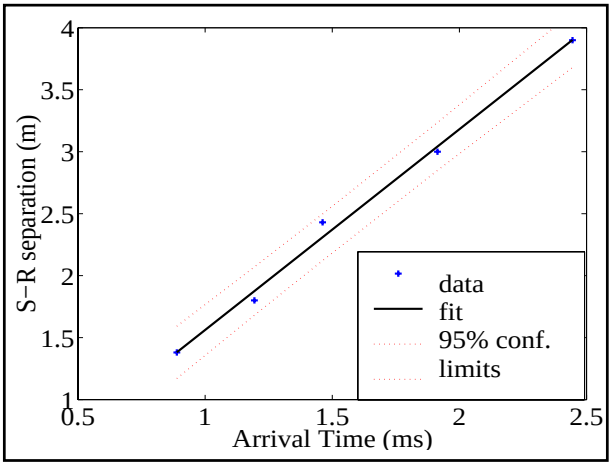

Figure 4. Plot of S-R separation against arrival time for 35 kHz, including least squares fit and 95% confidence limits.

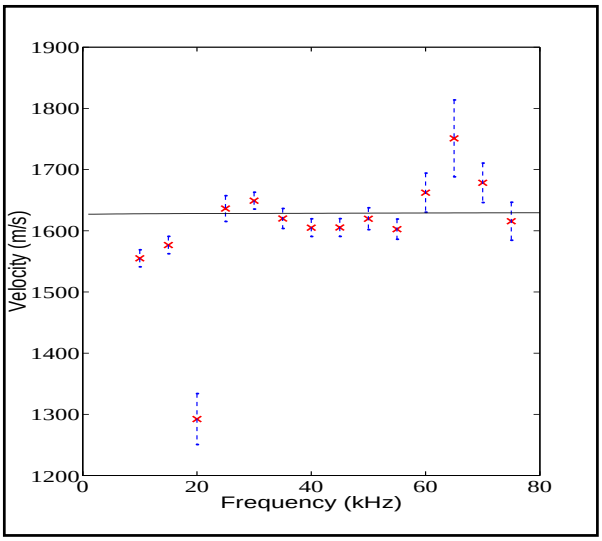

Figure 5. Frequency dependent velocity: measured velocities (X), with errors corresponding to 95% confidence limits, and fast wave velocity predicted by Biot model (black line).

The frequency dependent attenuation can be calculated from equation 1.

$$\ln(A) = -\alpha x + c. \qquad (1)$$

where A is the amplitude of the stacked-filtered-received wave, after correcting for geometric spreading, x is the S-R separation, α is the attenuation coefficient in Nepers/m and the parameter c represents the frequency response of the SPADE and receiver. At any fixed frequency, for all S-R separations, c will be constant.

Geometric spreading was calculated from water tank tests, with care taken to duplicate the field geometry. For each frequency, pressure spreading was modeled using $1/x^p$. Best-fit exponents p depended on frequency, varying from 0.72 to 0.91.

For each frequency *ln(A)* was plotted against S-R separation and a least squares linear fit applied, the negative of gradient of which represents the attenuation coefficient in Nepers/m, Fig. 6. The frequency dependent attenuation coefficient, in dB/m, is plotted in Figure 7. Amplitude data from signals that displayed poor transmitted waveforms were neglected. Attenuation data displayed in figure 7 are based on either three or more (X) or two (X) valid amplitudes.

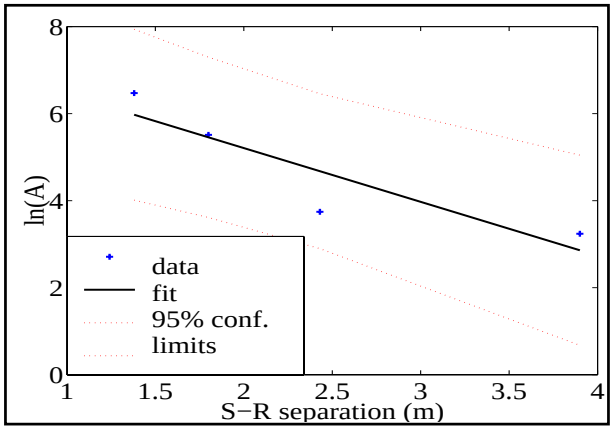

Figure 6: Plot of ln(A) against S-R separation for 35 kHz.

5. Biot Model

The compressional wave velocity and attenuation of the sediment was modelled using Biot theory [27, 28], which was implemented as described in [29]. Biot theory assumes that attenuation is solely due to viscous forces between the solid and the fluid and predicts two compressional waves: a fast wave and slow wave.

Grain size analysis revealed homogeneous medium/fine sand, with a mean grain size of 249 μm. Using feasible parameters for such sediment, observed velocities and attenuations could not be modelled using the slow compressional wave, with predicted velocities less than 150 m/s and attenuations greater than 100 dB/m. This implies that the observed signal corresponds to the fast wave, a phenomenon supported by [29].

A Biot model was applied using the following parameters, which are typical for a saturated, marine, medium/fine grained sand: porosity 42% [11]; permeability 100 mD; tortuosity 1.8; grain density 2650 kg/m^3; grain bulk modulus 36.5 GPa; water density 1024 kg/m^3; water bulk modulus 2.25 GPa; fluid viscosity 1 cP and mean pore radius 25 μm.

In the absence of shear wave velocities, a mean value, calculated *in situ* at 38 kHz for surface sands [25], of 120 m/s was used. This resulted in a frame shear modulus of 0.03 GPa. The frame bulk modulus was then adjusted to fit the fast wave velocity to the observed velocity, resulting in a best-fit value of 0.31 GPa. This is lower than values of 1.1-0.7 GPa predicted for medium/fine sands by figure 2 in [30]. Predicted fast wave velocity and attenuation are plotted in Figures 5 and 7 respectively.

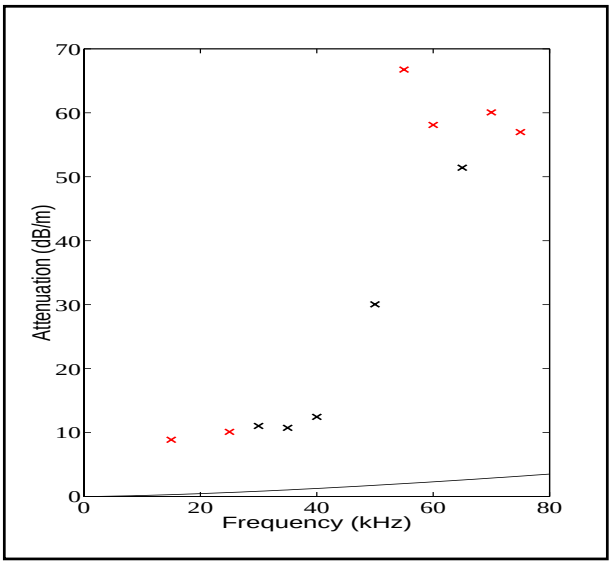

Figure 7. Frequency dependent attenuation: measured attenuations based on three or more amplitudes (X) and two amplitudes (X) and fast wave attenuation predicted by the Biot model (black line). Errors are omitted as they are less the 0.1 dB/m.

6. Discussion and conclusions

Neglecting the anomalous 20 kHz data, the observed velocity possesses a mean value of 1630 m/s. From 25 - 55 kHz velocities appear relatively constant, implying a non-dispersive medium over this frequency range. However a velocity peak from approximately 60 - 70 kHz and the presence of velocities less than the mean, at frequencies less than 20 kHz, suggest a dispersive medium over these ranges. No conclusions can be made for frequencies greater than 75 kHz. The model applied cannot account for the observed velocity variations. While Biot theory models phase velocity, the finite bandwidth of the emitted pulses results in the measured velocity strictly representing a group velocity. The use of tonal pulses ensures that the measured velocity will be a close approximation to the phase velocity at the pulse's central frequency. However, in dispersive media, these may differ.

Observed attenuation displays a gradual increase with frequency from 15 - 40 kHz. Between 40 and 50 kHz attenuation begins to increase sharply, reaching values of approximately 60 dB/m at 55 - 75 kHz. The scatter in the data at frequencies greater than 55 kHz arises from the majority of attenuations in this region being calculated from least square fits to only two data points. Such attenuations are suspect. The predicted fast wave attenuation is much smaller than that observed. This discrepancy may arise from the additional dissipation of energy from scattering and diffraction effects, which Biot theory does not consider. Observed results suggest that scatter is a dominant attenuation mechanism, the effects of which become more pronounced at higher frequencies. This is surprising as the mean grain size is at least a factor of 800 less than the smallest wavelength examined. Additional sources of this discrepancy may be the use of an uncertain spreading law (the use of spreading laws estimated in water assume that compressional wave velocity in water and sediment is the same) and heterogeneities in the sediments

Future work will include the use of finer frequency increments and the *in situ* calibration of the SPADE.

Acknowledgements

The authors would like to thank Martin Gutowski and Ronan Apprioual for their assistance with fieldwork and Ronan Apprioual for the grain size analysis. This work was funded by NERC studentship NER/S/A/2000/03621.

References

[1] F.N. Tullos and A.C. Reid: Seismic attenuation of Gulf Coast sediments, Geophysics **34** (1969) pp. 516-528.

[2] F. Collins and C.C. Lee: Seismic wave attenuation characteristics from pulse experiments, Geophysics **21** (1956) pp. 16-40.

[3] L. Hampton: Acoustic properties of sediments: an update, Reviews of Geophysics **23** (1985) pp. 49-60.

[4] F.J. McDonal *et al.*: Attenuation of shear and compressional waves in Pierre shale, Geophysics **23** (1958) pp. 421-439.

[5] N. Ricker: The form and laws of propagation of seismic wavelets, Geophysics **18** (1953) pp. 10-40.

[6] R.D. Stoll *et al.*: Field experiments to study seafloor seismoacoustic response, Journal of the Acoustical Society of America **89** (1991) pp. 2232-2240.

[7] P.S. Hauge: Measurements of attenuation from vertical seismic profiles, Geophysics **46** (1981) pp. 1548-1558.

[8] D. Rauch: Bottom-Interacting Ocean Acoustics, New York and London, Plenum Press 1980, pp. 307-327.

[9] E.L. Hamilton: Low sound velocites in high porosity sediments, Journal of the Acoustical Society of America **28** (1956) pp. 16-19.

[11] E.L. Hamilton: Sediment Sound Velocity Measurements made In Situ from Bathyscaph TRIESTE, Journal of Geophysical Research **68** (1963) pp. 5991-5998.

[11] E.L. Hamilton: Sound velocity and related properties of marine sediments, North Pacific, Journal of Geophysical Research **75** (1970) pp. 4423-4446.

[12] E.L. Hamilton: Compressional-wave attenuation in marine sediments, Geophysics **37** (1972) pp. 620-646.

[13] R.H. Wilkens and M.D. Ricardson: The influence of gas bubbles on sediment acoustic properties: in situ, laboratory, and theoretical results from Eckernforde Bay, Baltic sea, Continental Shelf Research **18** (1998) pp. 1859-1892.

[14] M.D. Richardson *et al.*: The effects of free-methane bubbles on the propagation and scattering of compressional and shear wave energy in muddy sediments, Journal of the Acoustical Society of America **95** (1994) pp. 3218.

[15] M.D. Richardson, A. Jim, and C. Bob: Overview of SAX99: Environmental Considerations, IEEE Journal of Oceanic engineering **26** (2001) pp. 26-53.

[16] A.L. Anderson and L. Hampton: Physics of sound in marine sediments, New York and London, Plenum 1973, pp. 357-371.

[17] D.J. Shirley and A.L. Anderson: In situ measurement of marine sediment acoustical properties during coring in deep water, IEEE Transactions on Geoscience Electronics **GE-13** (1975) pp. 163-169.

[18] A.B. Wood and D.E. Weston: The propagation of sound in mud, Acustica **14** (1964) pp. 156-162.

[19] C. McCann and D.M. McCann: The attenuation of compressional waves in marine sediments, Geophysics **34** (1969) pp. 882-892.

[20] A. Turgut and T. Yamamoto: Measurements of acoustic wave velocities and attenuations in marine sediments, Journal of the Acoustical Society of America **87** (1990) pp. 2376-2383.

[21] N.L. Frazer and S. Fu: Seabed sediment attenuation profiles from a movable sub-bottom acoustic vertical array, Journal of the Acoustical Society of America **106** (1999) pp. 120-130.

[22] A.I. Best, Q.J. Huggett, and A.J.K. Harris: Comparison of in situ and laboratory acoustic measurements on Lough Hyne marine sediments, Journal of the Acoustical Society of America **110** (2001) pp. 695-709.

[23] M.D.J. Tuffin *et al.*: *Temporal variability in P-wave attenuation due to gas bubbles in a marine sediment*, Proceedings of the Institute of Acoustics Volume 23 Part 2,Southampton Oceanography Centre, 2001, pp. 283-298

[24] A.I. Best, J.A. Roberts, and M.L. Somers: A New Instrument for Making In-Situ Acoustic and Geotechnical Measurements in Seafloor Sediments, Journal of the Soc-iety for Underwater Technology **23** (1998) pp. 123-131.

[25] E.I. Thoros *et al.*: *An experiment in high-frequency sediment acoustics: SAX99*, Proceedings to the Institute of Acoustics Volume 23 Part 2,Southampton Oceanography Centre, 2001, pp. 344-354

[26] R.D. Stoll: Velocity-dispersion in water saturated granular sediment, Journal of the Acoustical Society of America **111** (2002) pp. 785-793.

[27] M.A. Biot: Theory of propagation of elastic waves in a fluid saturated porous solid, part 1, Journal of the Acoustical Society of America **28** (1956) pp. 168-178.

[28] M.A. Biot: Theory of propagation of elastic waves in a fluid saturated porous solid, part 2, Journal of the Acoustical Society of America **28** (1956) pp. 179-191.

[29] A.I. Best: PhD Thesis, University of Reading 1992, pp. 201-222.

[30] E.L. Hamilton: Elastic properties of marine sediments, Journal of Geophysical Research **76** (1971) pp. 579-604.